Protein Engineering, Design & Selection

An Efficient Method for Enzyme Immobilization evidenced by Atomic Force Microscopy

C. Marcuello [1*], R. de Miguel [1*], C. Gómez-Moreno [1,2], M. Martínez-Júlvez [2,3] and A. Lostao [1,4^]

1 Laboratorio de Microscopías Avanzadas, Instituto de Nanociencia de Aragón, Universidad de Zaragoza, 50018 Zaragoza, Spain
2 Departamento de Bioquímica y Biología Molecular y Celular, Universidad de Zaragoza, 50009 Zaragoza. Spain
3 Institute of Biocomputation and Physics of Complex Systems (BIFI), 50018 Zaragoza and BIFI-RocaSolano CSIC Joint Unit, Spain
4 Fundación ARAID, 50018 Zaragoza, Spain

* Both authors contributed equally to this work

^ Corresponding author: Anabel Lostao, Laboratorio de Microscopías Avanzadas (LMA), Instituto de Nanociencia de Aragón (INA), Universidad de Zaragoza, Ed. I+D+i. Campus Río Ebro. 50018 Zaragoza, Spain
FAX: 0034976762776; e-mail: aglostao@unizar.es

Running title:
Efficient enzyme immobilization evidenced by AFM

Abstract

Immobilization of proteins in a functionally active form and proper orientation is fundamental for effective surface-based protein analysis. A new method is presented for the controlled and oriented immobilization of ordered monolayers of enzymes whose interaction site had been protected using the protein ligand. The utility of this method was demonstrated by analyzing the interactions between the enzyme Ferredoxin-$NADP^+$ Reductase (FNR) and its redox partner Ferredoxin (Fd). The quality of the procedure was deeply evaluated through enzymatic assays and Atomic Force Microscopy. Single-Molecule Force Spectroscopy revealed that site-specifically targeted FNR samples increased the ratio of recognition events 4-fold with regard to the standard randomly-modified FNR samples. The results were corroborated using the cytochrome *c* reductase activity that gave an increase on surface between 6-12 times for the site-specifically targeted FNR samples. The activity in solution for the enzyme labelled from the complex was similar to that exhibited by wild-type FNR while FNR randomly tagged showed a 3-fold decrease. This indicates that random targeting protocols affect not only the efficiency of immobilized proteins to recognize their ligands but also their general functionality. The present methodology is expected to find wide applications in surface-based protein-protein interactions biosensors, single molecule analysis, bioelectronics or drug screening.

Keywords: atomic force microscopy / enzyme / immobilization / molecular recognition / protein interaction

Funding

This work was supported by the Spanish Ministerio de Educación y Ciencia [grant number BIO2006-09178-C02]; Ministerio de Ciencia e Innovación [grant number BIO2010-14983]; the regional Gobierno de Aragón and MICINN-FEDER [grant B18 Biología Estructural] and ARAID [grant to A.L.].

Introduction

Protein immobilization is a decisive step in the surface-based analysis consisting of protein-protein (or ligand) interactions. In the last years many research lines have been devoted to establish stable and strong protein attachment onto different kinds of surfaces to develop microarray-based proteome analysis (MacBeath and Schreiber, 2000; Tao and Shu, 2006; Kwon *et al.*, 2006; Rodriguez-Devora *et al.*, 2011); single molecule studies (Deniz *et al.*, 2008; Roy *et al.*, 2008); biochips (Hong *et al.*, 2005; Borisov and Wolfbeis, 2008); drug screening (Cooper *et al.*, 2002; Sevecka and MacBeath, 2006; Wolf-Yadlin *et al.*, 2009) and bioelectronics (Willner *et al.*, 2000; Heller, 2004; Amstrong, 2005; Leger and Bertrand, 2008). Due to their versatility and functions, proteins are the most generally used biomolecules in technological devices. Among protein immobilization protocols, those designed for antibodies and enzymes stand out. It is crucial to develop methods for the adequate biofunctionalization which will confer the appropriate features for biotechnological and biomedical applications. Several strategies for linking antibodies onto surfaces have been described, a part of them anchoring the molecules in an oriented manner through the Fc regions, leading to a more efficient interaction with the antigens (Jung *et al.*, 2008; Ikeda *et al.*, 2009; Kausaite-Minkstimiene *et al.*, 2010). Nevertheless, only a few strategies for linking proteins in an oriented manner have been proposed at the present time, based on electrostatic interactions (Wang *et al.*, 2006), through the integration on lipidic layers (Gutierrez-Sanchez *et al.*, 2011), or introducing specific residues through site-directed mutagenesis (Huang *et al.*, 1997; Hernandez and Fernandez-Lafuente, 2011).

Enzymes are versatile biocatalysts that offer high stereo-specificity towards chemical and biochemical reactions providing essential products for living organisms. However, their lack of long-term stability together with the difficulty to recover and recycle them when used in solution, have limited their applications. These problems may be overcome by the immobilization of the enzymes onto surfaces (Bornscheuer *et al.*, 2003). The main challenge in enzyme immobilization is maintaining the catalytic activity, that is, to avoid their denaturation and controlling the proper orientation of the immobilized enzyme to ensure the access of the enzyme substrate (or ligand) to the active or binding site (Garcia-Galan *et al.*, 2011). Most immobilization procedures do not actively control the orientation of the enzymes, hence making inevitable the burying and inaccessibility of their active site. This could account for the dramatic decrease in activity often observed when an enzyme is immobilized on a surface.

Atomic Force Microscopy (AFM) is the only microscopic technique able to visualize biomolecules at the single-molecule level with sub-nanometer accuracy in liquid (Binning *et al.*, 1986). It allows studying the topology, adhesion, elasticity, association processes, dynamics and other properties of biological samples. In the Single-Molecule Force Spectroscopy (SMFS)

mode of an AFM system, the cantilever deflection is recorded as a function of the vertical displacement of the piezo scanner. SMFS offers the possibility of performing quantitative analysis of ligand–receptor interactions allowing addressing questions about the nature and magnitude of forces and the related binding energy landscape (Florin *et al.*, 1994; Merkel *et al.*, 1999). The AFM probe consists of a microfabricated cantilever that behaves as a spring and ends in a sharp nanotip that can be moved in three dimensions with subnanometer accuracy thanks to several piezoelectric scanners. The tip is brought near the sample surface so that forces acting on the tip cause the cantilever to bend. A laser beam is aimed at the top of the cantilever and reflected onto a photodiode. By attaching one of the interacting molecules to the AFM tip and the other molecule to the sample surface, the molecular binding forces can be quantified from the positive binding/rupture events. Jumping mode (JM) is a force-scan based AFM mode where simultaneous topographic and tip–sample adhesion maps are acquired (de Pablo *et al.*, 1998). This approach can be operated in such a way that the unbinding forces between receptor molecules on a sample and a ligand suitably attached to the AFM tip can be obtained from the adhesion images (Sotres *et al.*, 2008).

The protein ligand, Ferredoxin (Fd), that binds specifically to the surface of the enzyme Ferredoxin-$NADP^+$ reductase (FNR), was used to prove the general applicability of the strategy here proposed and its utility for the development of more efficient bioactive surfaces. In the cyanobacterial physiological reaction two Fd molecules interact sequentially with FNR for the step-wise transfer of two electrons (Jelesarov and Bosshard, 1994). In iron-deficient cultures Fd cannot be synthesized and is replaced by the FMN-containing Flavodoxin (Fld) that is also a redox partner for FNR (Rogers, 1987; Fillat *et al.*, 1988). Fld binds the same interaction surface in FNR and achieve the same role as Fd (Martínez-Júlvez *et al.*, 1999). Finally, reduced FNR will be used to reduce $NADP^+$ to NADPH (nicotinamide adenine dinucleotide phosphate). The formation of a transient complex between Fd and FNR is required for the electron transfer, and extensive studies have been reported to characterize such protein–protein interaction (Medina and Gómez-Moreno, 2004; Peregrina *et al.*, 2010; Peregrina *et al.*, 2012).

Most of the immobilization strategies described in the literature consists of long procedures comprising many preparatory steps that are optimized for a specific functionalization of the protein surface. Nevertheless, efficient, easy and universal methodologies for the immobilization of functional and oriented proteins onto surfaces are still lacking. Herein, we propose the functionalization of the protein-protein (or ligand) complex, followed by a one-step separation and immobilization on a flat surface. The strategy takes advantage of the reversible interactions between the protein and the ligand. By using this strategy, the binding site of the enzyme is protected from crosslinking thus allowing a site-directed covalent attachment facing the binding site upward to the ligand, leading to a more efficient molecular recognition and interaction. In the present paper, the functionality and proper orientation of FNR to Fd is

demonstrated through the cytochrome *c* reductase activity assay, SMFS and molecular recognition imaging.

MATERIALS AND METHODS

Protein labelling and separation of tagged species

Recombinant FNR, Fld and Fd proteins from *Anabaena* were purified from *E. coli* cultures containing recombinant DNA as previously described (Fillat *et al.*, 1991; Martínez-Júlvez *et al.*, 2001). FNR was modified on its surface in two different conditions: in the first case, the FNR enzyme was mixed with Fd in a molecular ratio of 1:2. In the other case the solution contained only FNR. In both cases the protein solutions were incubated for 30 min at room temperature with 15 µl of 20 mM sulfosuccinimidyl 6-(3'-[2-pyridyldithio]-propionamido) hexanoate (Sulfo-LC-SPDP; Pierce) in order to form stable amide bonds through the lysine residues of proteins and the amine-reactive N-hydroxysuccinimide (NHS) ester of the heterobifunctional crosslinker. This reaction produces tagged-species of the FNR:Fd complex, and the free enzyme FNR, respectively, carrying all species a C_9-long arm containing a pyridyl-dithiopropionyl reactive group (PDP). Reaction on complex FNR:Fd will yield FNR molecules whose surfaces will be coated by the PDP tag, except in the interface area covered by the protein partner. The same will occur for the Fd molecule from the complex (these species will be called throughout the paper FNR_c-PDP and Fd_c-PDP, respectively). In the second case, when FNR was incubated alone with the crosslinker, the protein surface will be randomly-coated by the tag, including the Fd-interaction area (this species will be called throughout the paper FNR_r-PDP). The complex [FNR_c:Fd_c]-PDP was treated with 500 mM NaCl for 10 minutes at 4 ºC to favour complex dissociation. [FNR_c:Fd_c]-PDP was dissociated in FNR_c-PDP and Fd_c-PDP and isolated by size exclusion chromatography using a Superdex 75 column (GE Healthcare) in 50 mM Tris-HCl, 250 mM NaCl, pH 8. FNR_r-PDP was purified using Sephadex G-25 desalting chromatography (GE Healthcare) in 50 mM Tris-HCl. The purity of fractions was checked by SDS-PAGE with gradient 8-25 % in a PhastSystem (GE Healthcare) using a Low Molecular Weight Market kit as reference (GE Healthcare).

Immobilization of FNR on mica

Cleaved muscovite mica pieces (Electron Microscopy Sciences) were exposed to vapours of 3-Aminopropyl)triethoxysilane (APTES; Sigma-Aldrich) and N,N-Diisopropylethylamine (Hünig's base; Sigma-Aldrich) in a ratio of 3:1 in volume for 2 h under argon atmosphere. 20 mM Sulfo-LC-SPDP in PBS-EDTA-azide (phosphate buffered saline; ethylenediaminetetraacetic acid; Pierce) was added to the aminated mica for 50 min at room temperature. The exposed PDP groups were reduced to sulfhydryl groups by adding freshly

prepared 150 mM dithiothreitol (DTT; Sigma-Aldrich) in PBS-EDTA-azide stirring for 30 min at 4 ºC. FNR_c-PDP or FNR_r-PDP, carrying a disulfide group in the PDP tag, were incubated with the thiol–containing mica pieces and stirred for 18 hours at room temperature to allow the formation of disulfide bonds between them. Unbound protein was removed washing three times with PBS, 0.2 % Tween 20 (Panreac), 0.1 % sodium dodecyl sulphate (SDS; Panreac) for 30 min under mild stirring. Different concentrations of the tagged proteins were used in order to get the adequate amount of FNR molecules on the mica surface to form a saturated monolayer.

AFM tip functionalization

Silicon nitride AFM cantilevers were functionalized with maleimide-terminated flexible polyethylene glycol (PEG) linkers (MW 3400) (Novascan Technologies Inc, Ames, USA). The modified cantilevers had nominal spring constants of 0.01 and 0.03 N/m (V-shaped) and 0.02 N/m (rectangular shape) with integrated pyramidal tips. Cantilevers were calibrated using the thermal noise method (Hutter and Bechhoefer, 1993). Fd_c-PDP was treated with 50 mM DTT for 30 minutes at room temperature in order to expose thiol groups on the Fd surface. The cantilevers were incubated with 42 μM thiolated-Fd in PBS-EDTA, pH 7.0, for 1 hour and washed three times to remove the excess of reactants. In this case only tagged-Fd isolated from the previously formed [FNR_c-Fd_c] complexes was used.

Force Spectroscopy

AFM measurements were performed with a Cervantes Fullmode SPM (Nanotec Electrónica S.L, Tres Cantos, Spain). The system was used in the SMFS mode to obtain force-distance cycles for Fd-cantilever/FNR-mica interactions. Force-distance curves were obtained applying a voltage to the z-piezo at a velocity of 1.9 μm s^{-1}. Several hundred curves were taken for each type of sample. Negative control experiments were carried out blocking available FNR sites by incubating the sample with excess free Fld in a concentration of 706 μM for 15 minutes yielding a significant decrease in the binding interaction between the cantilever and the sample surface.

Atomic Force Microscopy Imaging

AFM images were taken in the Jumping Mode (JM) operation that allows mapping the topography and adhesion of the sample simultaneously (de Pablo *et al.*, 1998). The forces applied to the sample are precisely controlled preventing soft samples to be damaged (Sotres *et al.*, 2007). V-shaped silicon nitride cantilevers with integrated pyramidal tips and spring constants of 0.01-0.03 N/m were employed (Bruker Probes, MSCT-Micro lever Probes). Levers cleaning and image obtaining with the JM was carried out as described elsewhere (Sotres *et al.*, 2007). Image processing was performed with WSxM software (Horcas *et al.*, 2007). Measurements were conducted in PBS at 20 °C. Recognition Images were taken using JM at

low applied forces as previously described (Sotres *et al*., 2008) with the Fd_c-functionalized tips. In order to appreciate molecular recognition at the single molecule level FNR samples with separated molecules were required. For this purpose, different concentrations of FNR were incubated on mica until the adequate results were obtained. Blocking of the FNR interaction sites in the sample was made in the same way as for SMFS measurement controls. Images of the blocked samples were also taken with JM.

Steady-State Enzymatic Assays

The functionality of the tagged-proteins both immobilized and in solution was verified using the cytochrome *c* reductase activity. In this assay an electron transfer process takes place between a molecule of NADPH and one of cytochrome *c* through the formation of a FNR:Fd or FNR:Fld complex (Medina *et al*., 1998). This activity was assayed with the two types of PDP-labelled enzyme (FNR_c-PDP and FNR_r-PDP). The activity of FNR immobilized on mica was measured using a Synergy HT Sheet Reader system (Biotek). The standard reaction mixtures contained, in a final volume of 1.165 mL, 100 μM Fld, 0.71 mM horse cytochrome *c* and 190 μM NADPH in 50 mM Tris-HCl, pH 8.0. Assays were performed in 6-well plates with immobilized-FNR 2.0 x 2.0 cm mica pieces at the bottom. One of the 6 wells contained no mica while in other a treated but without FNR mica piece was placed, using both as references. All premixed reagents, except NADPH, were added to each well and, after 60 s, 110 μL of a 2 mM NADPH solution were added in each one. After 5 seconds of stirring, the absorbance at 550 mM was recorded every 10 s on the different mica sheets until the redox reaction finished. An increase of absorbance was observed in all wells where the reaction took place. Tagged-enzymes were also assayed in solution using quartz cuvettes adding 4 nM FNR in the same final volume and reagent concentrations as above using a Cary 100Bio spectrophotometer (Varian). Control activity measurements were also made using a final concentration of 4 nM wild-type (wt) FNR. Reagents were purchased from Sigma-Aldrich.

Estimated quantification of immobilized FNR

An estimation of the amount of enzyme molecules (36 kDa globular protein) that can be immobilized on a flat mica surface, forming a monolayer, was worked out considering that the FNR molecule diameter (taken from PDB 1QUE) is 61 Å and that 70 Å is the intermolecular average distance between two FNR molecules in these samples (obtained from topography AFM images from saturated samples). With all these premises the estimated FNR amount immobilized on a 2.0 x 2.0 cm mica piece was calculated to be 0.139 μg.

Results

Protein tagging and functionalization

For the covalent immobilization of FNR on the mica surface, both elements were functionalized with the same heterobifunctional crosslinker. Previously, the mica sheets were aminated with APTES in gaseous phase to obtain a monolayer of reactive amino groups (Lyubchenko *et al.*, 2009). These groups reacted with the SPDP crosslinker, generating a thiol layer after a reduction treatment. Incubation with the enzyme produced homogeneous layers of molecules via disulfide bonds. FNR was modified by the SPDP reagent either in the presence of the protein partner Fd, in which case the interaction area would be protected, and in the absence of the iron protein, that would lead to an unspecifically modified protein. Figure 1 shows the results for the separation in a single chromatography step of the tagged proteins obtained after modification while forming a complex. The identity and purity of both FNR_c-PDP and Fd_c-PDP was checked by SDS-PAGE (see inset in Figure 1). FNR_r-PDP was collected pure after desalting through a Sephadex G-25 matrix (results not shown).

Steady-State Enzymatic Assays of free and immobilized FNRs

The different mica samples carrying bound FNR were assayed using the cytochrome *c* reductase activity assay upon addition of NADPH. The preparation of FNR-functionalized mica pieces required the previous calibration of the optimal amount of enzyme to be used during the immobilization procedure. Results in Figure 2 indicate that the highest enzymatic activity of the functionalized mica was obtained when approximately 1 μg of FNR_c-PDP per cm^2 was used. Experimental quantification of total amount of immobilized enzyme on mica was analyzed by a microBCA assay (results not shown) by taking into consideration the amount of FNR used in immobilization and subtracting the quantity not fixed on mica and released during the washing. This methodology did not result adequate because the free sulfhydryl groups on the surface of mica interfere with the cupper ions present in the test producing an overestimation of the sample. Therefore, the estimated quantification of immobilized enzyme was performed as described in Materials and Methods. Table I shows the parameters obtained for the cytochrome *c* reductase activity with different amounts of incubated enzyme. Fld was used as electron acceptor in the cytochrome *c* reductase activity assays. The use of Fld, instead of Fd, is due to the easier availability to this protein and to the fact that both proteins interact at the same site in FNR (Martínez-Júlvez *et al.*, 1999). It is observed that the enzymatic activity increases as higher amounts of FNR are incubated on the functionalized mica sheets reaching a maximum value of around 1-3 μg FNR. This is an interesting result since it probes the functionality of the enzyme bound by this procedure. Further increase in the amount of enzyme produces lower activities, suggesting that immobilization of higher amounts of enzyme on the mica sheets produces steric hindrance on the enzyme. This could be due to the higher accessibility of the immobilized

enzyme to interact with protein components of the assay when the immobilized enzyme is far away from other molecules on the surface. In Table I the activity of the FNR_r-PDP immobilized on the mica surface is also presented. These values are clearly lower than those obtained for FNR_c indicating the inefficiency of the random strategy.

To check the integrity of the tagged species of FNR, the cytochrome *c* reductase activity in solution of these FNR species was compared with that obtained for the wt enzyme as a reference. The activity was measured both using a spectrophotometer and also a sheet reader. The results were similar in both cases. Wt-FNR and FNR_c-PDP enzymes exhibited turnover numbers (TN) values of 17.3 and 18.3 s^{-1}, respectively, while FNR_r-PDP showed a rate of 5.5 s^{-1}. All measurements were performed with 4 nM enzyme that is the concentration normally used for measuring FNR activity in solution (Medina *et al.*, 1998). These results not only ensure the functionality of FNR_c-PDP, but also assert that preserving the interaction surface of FNR free of the covalent tag is a requirement for full activity of the enzyme. On the contrary, this result shows that the random labelling strategies decrease the capabilities of the enzymes to recognize and bind efficiently its protein partners in a major proportion. In this particular enzymatic system, the turnover number using the random labelled FNR with respect to the FNR tagged from the complex decreases by more than 3 times.

AFM imaging

AFM was used as a tool to detect the results of the immobilization procedure of FNR on the surface of a mica sheet at the molecular level. The topography images showed that the enzyme forms a homogeneous monolayer bound to the thiolated surface (Figure 3c). Moreover, the images taken on the APTES-mica samples gave heights of around 0.6 nm (Figure 3a, b). It agrees with previous published data suggesting lengths for APTES attached to mica in aqueous media of 0.6-0.9 nm (Volcke *et al*., 2010) and 0.6 nm for non-hydrolyzed APTES (Zhu *et al*., 2012). It can be appreciated that the mica sheets are densely covered by hydroxyl groups although certain areas of the surface show empty spaces which indicates that the reaction has not modified the surface. The thiolated mica showed also homogeneous layers, and the height increases to approx. 1 nm in the topography image (Figure 3c, d). Topology images of the surface functionalized with FNR_c-PDP show a height between 8-14 nm (Figure 3e, f). Very similar results were obtained for FNR_r-PDP samples (not shown). The height coincides with the expected length for the product of the covalent reaction between FNR-PDP and the thiolated APTES formed on the mica surface. It is worth to mention that the layer, as imaged by AFM, is not regular but it rather displays mounts and valleys randomly distributed over the surface.

Force spectroscopy

The total adhesion peaks generated during each Force-distance curve either originates from a specific interaction (formation of a FNR–Fd bond) or from a non-specific one of any other origin. An important advance in SMFS came with the use of spacers that increased the length and flexibility of the sensor, allowing the ligand to freely move around the tip favoring receptor recognition and identification of the specific forces (Hinterdorfer *et al.,* 1996). Among them, PEG tethers present an especially attractive system because of their feature-rich stretching profile in water, so that these specific peaks show a nonlinear parabolic-like shape which is characteristic of the stretching of a PEG linker. The flexible tether sustains the increasing force until the complex dissociates, as indicated by a sudden jump to zero normal force. This occurs at a certain force value (unbinding or rupture force) and tip–sample distance (rupture length). In contrast, in non-specific adhesions the contact curve extends towards negative values keeping the same slope, which indicates that whatever the origin of this interaction is, the bare tip remains in contact with the surface. Moreover, this excludes participation of the sensor. In our system, once the FNR molecules are immobilized onto the AFM liquid chamber and the cantilever probe is functionalized with Fd_c, force spectroscopy experiments can be performed since this is an appropriate technique for studying the interaction forces. Figure 4a shows a typical mica-FNR_c:Fd_c-tip force scan obtained when the functionalized tip of an AFM microscope is approached to an interacting surface. Departing from the 0-force point, the tip can be moved closer to the sample with an increase in force (dashed line). Once the tip reaches the surface, pushing it further towards the sample requires higher (positive) forces since a collapse between the two molecules is taking place. Retraction of the tip produces an increase in the (negative) force that goes to an unbinding force of 26 pN (f_u) (solid line). Then a sharp jump is observed indicating that a sudden release has occurred between the tip and the sample. That is due to the rupture of the bond between the two interacting molecules. This force can be attributed to a specific event that occurs at a specific rupture length (l_u) coincident with the maleimide-PEG linker stretched size used to attach Fd to the tip. Furthermore, the extension trace of the curve preceding the jump-off-contact coincides with the stretching curve of a flexible PEG spacer that follows a worm-like chain model (Marko *et al.,* 1995).

In Force spectroscopy experiments the efficiency of the binding between the tip and the sample can be determined from the number of specific rupture events that occur after typically several hundred approaches. In the analysis, only those force curves that showed at least a specific rupture event were taken as positive, being those peaks that meet the specific conditions described in the preceding paragraph, meanwhile approaches are the total curves registered. The fact that the force curves taken on samples blocked with Fld gave peaks –though in a lower proportion- at the same rupture length and rupture force that the taken on non-blocked samples also ensures the specificity of the measurements. Figure 4b shows the

summary of the force spectroscopy results obtained approaching Fd_c-functionalized tips to FNR_c and FNR_r samples on mica at a certain loading rate, 19.5 nN s^{-1}. The conclusion is that 61 % of the approaches between the tip and the oriented samples produced specific rupture events. The results clearly show that this number decreases drastically when the randomly immobilized FNR samples are used. In this case only a 17 % of the approaching events are observed to produce binding. This data is similar to those obtained for the typical SMFS measurements where standard functionalization protocols are used. This is an interesting result since it provides direct evidence that the AFM measured force comes from the interaction between the two partner proteins and also that this is an specific binding produced through the recognition of the specific area in FNR that is protected by Fd during the preparation of the FNR_c-PDP species. Moreover, Figure 4b also indicates that the efficiency of the binding events obtained for the FNR_c-mica samples drops to a level similar to that of the randomly modified sample when the site for that interaction is blocked (approx. 14 %) when the FNR_c sample is incubated with a high excess of the partner protein, Fld.

Molecular Recognition Imaging

Images of the recognition events between the two interacting proteins can be obtained directly by AFM scanning. Using a Fd- modified tip and operating in the Jumping Mode, it is possible to obtain simultaneously both a topography image, that corresponds to the scanning of the deposited sample profile, and an adhesion image, taken from the points where maximum adhesion force between tip and sample are obtained. This is based on the fact that non-specific tip-sample interactions are minimized when operating in a repulsive regime at low applied forces (Sotres *et al*., 2008). This produces images showing mainly the specific forces between the molecules in every pixel. Topographical images of Figure 5 show several features that can be attributed to single FNR molecules. The measured protein diameter is around 25 nm, much larger than the known 6 nm diameter of FNR. This discrepancy is due to the tip dilation effect, always present in AFM imaging. Our results show that the adhesion images correlate quite well with the topography images in the case of the oriented samples (Figure 5a, b). There is a close correspondence between the observation of a molecule in the topology map and the simultaneous increase of the adhesion force at the same position. As it is clear from the topographic image of Figure 5a, tip functionalization does not prevent the observation of the protein molecule and molecular resolution hardly suffer from this functionalization when compared with a bare tip. When these samples are blocked with Fld the adhesion images show an important decrease in the number of specific events (Figure 5c, d) in a similar extension to the images corresponding to the randomly tagged enzymatic samples (Figure 5e, f). It is clear that the high adhesion peaks on top of the molecules seen in the topography map of Figure 5c disappear after blocking, as it is shown in its respective simultaneous adhesion map in Figure

5d. This is indicative of the specificity of the measurements. The larger size exhibited by the molecular features in Figure 5c is due to the addition of Fld on the immobilized sample which forms complexes FNR:Fld, bigger than single FNR molecules imaged in a and e. The features of both maps are a little displaced because they are produced by two different sensors. Adhesion is probed by the flexible PEG crosslinker that ends in a protein and presents several degrees of motion, while the topography sensor is the rigid tip apex. It is also noticeable that the adhesion peak width is narrower than the corresponding one in topography. This can be also attributed to the smaller size of the sensor probe with regard to that of the tip radius. This effect can cause a better resolution of molecules in the adhesion image than the obtained in the corresponding topology map.

Discussion

A strategy for the oriented immobilization of the enzyme FNR towards its protein partner onto silicon surfaces in a fully active form has been designed. The procedure takes advantage of the reversible character of protein-protein complexes that allows the functionalization of any part of the surface of a protein, except the interface area that is protected from crosslinker binding. Standard functionalization procedures introduce reactive groups over the whole protein structure covering essential interaction surfaces or binding pockets through the modification of important residues that could be involved in the recognition process. In the case of enzymes, these massive modification procedures not only diminish the probability of proper recognition between partner proteins, but also a decrease in the catalytic activity. In this work an enzyme has been immobilized in an oriented manner using a covalent procedure that preserves its functionality and leads to the assemblage of a homogeneous layer. It has been demonstrated that indiscriminate functionalization processes can modify the catalytic site of an enzyme. This alternative bio-conjugation process even improves the catalytic properties of enzymes and also the number of specific events in SMFS measurements. The same conclusions have been evidenced in the adhesion-recognition AFM images using functionalized Fd-tagged tips, obtaining an optimum correlation between the features in topography and adhesion images in oriented FNR samples. This correlation is pauperized in the cases of coverage with random and blocked FNR_c samples.

The conjugation strategy described in this work can be applied as a general methodology for those proteins that need to be oriented towards their protein partners with which they form a reversible complex. These results illustrate that the procedure described in this paper offers a double benefit, on one side it allows the immobilization of enzymes in a functional and oriented way, as has been demonstrated by the enzymatic assays and AFM images; on the other side, oriented immobilization of molecules becomes a procedure that substantially enhances the quality of SMFS experiments to analyze the mechanostability of protein complexes. The quality

in force spectroscopy measurements is proportional to the ratio of successful events with respect to the total number of approaches; so that a higher proportion reduces the error associated to the standard measurements when random immobilization procedures are used, producing low efficiency ratios of about 5-20 %. In the other hand, by using a force-scan based imaging mode as JM and choosing carefully the experimental conditions we have obtained spatially resolved ligand unbinding events maps on single enzyme molecules. This method opens the door to the development of very sensitive surface biosensors.

The strategy described here for measuring the interaction forces between proteins forming functional transient complexes could allow the correlation between mechanical forces stabilizing the complexes and their chemical stability as determined by the equilibrium constants. The present work also illustrates that it is possible to detect the binding force between two proteins that bind together for exchanging electrons. A reasonable strategy would be to compare the affinity of a protein for its partner depending on the state of its interaction surface. A non-modified surface would lead to efficient interaction while chemical modification of this surface would impede binding. This is not a straight forward issue but it could be approached by comparing the data obtained using alternative partner proteins (Fd and Fld), as well as those obtained with large number of protein mutants that our group has generated for biochemical and structural studies of protein-protein electron transfer reactions. Further work will be performed in this area.

As a summary, in this work the enzyme FNR was immobilized on a silicon substrate facing up the protein ligand recognition surface through decorating the protein complex with a crosslinker. Such tagged-proteins were separated from the complex in one-step purification. The enzyme was covalently attached to thiolated-mica and showed its capability to form homogeneous layers as checked by AFM imaging. The functionality was clearly demonstrated by specific activity assays. In such an immobilization, the recognition interface of the enzyme is faced toward the solution rather than toward the surface as was evidenced by enzymatic assays, SMFS and molecular recognition imaging; all these methods requiring the same specific orientation. Analysis of ligand binding using the specific cytochrome *c* reductase assays revealed that oriented enzyme samples resulted in about a 3-fold higher activity in solution and in a greater extent on surface, between 6-12 times in some cases and not quantifiable in the most of them, than random bound samples. Nanomechanical analysis of Fd binding using SMFS revealed that oriented FNR increased also the ratio of recognition events in about a 4-fold extension with respect to randomly bound FNR. The strategies for protein immobilization usually display a random character, which can produce an important inefficiency in the recognition purposes for which they were designed. Efficiency has an increased importance for the next future where miniaturization will grow progressively. The proposed methodology can

be very suitable for more sensitive and selective protein-protein surface-based studies, single molecule analysis, biosensors, drug screening and enzyme-based bioelectronics processes.

Acknowledgements

C. Marcuello and R. de Miguel thank DGA and MICINN for receiving a FPI and FPU fellowships, respectively. A. Lostao thanks ARAID for financial support. The authors also thank Iñigo Echániz for technical support.

References

Amstrong,F.A. (2005) *Curr. Opin. Chem. Biol.*, **9**, 110–117.

Binning,G., Quate,C.F. and Gerber,C. (1986) *Phys. Rev. Lett.*, **56**, 930–933.

Borisov,S.M. and Wolfbeis,O.S. (2008) *Chem. Rev.*, **108**, 423–461.

Bornscheuer, U.T. (2003) *Angew. Chem. Int. Edit.*, **42**, 3336-3337.

Cooper,M.A. (2002) *Nat. Rev. Drug Discov.*, **1**, 515–528.

Deniz,A.A., Mukhopadhyay,S. and Lemke,E.A. (2008) *J. R. Soc. Interface*, **5**, 15–45.

De Pablo,P., Colchero,J., Gómez-Herrero,J. and Baró,A.M. (1998) *Appl. Phys. Lett.*, **73**, 3300-3302.

Fillat,M.F., Borrias,W.E. and Weisbeek,P J. (1991) *Biochem. J.*, **280**, 187-191.

Fillat,M.F., Sandmann,G. and Gómez-Moreno,C. (1988) *Arch. Microbiol.*, **150**, 160-164.

Florin,E.L., Moy,V.T. and Gaub,H.E. (1994) *Science*, **264**, 415–417.

Garcia-Galan,C., Berenguer-Murcia,A., Fernandez-Lafuente,R. and Rodrigues,R.C. (2011) *Adv. Synth. Catal.*, **353**, 2885–2904.

Gutierrez-Sánchez,C., Olea,D., Marques,M., Fernández,V.M., Pereira,I.A.C., Vélez,M. and De Lacey,A.L. (2011) *Langmuir*, **27**, 6449–6457.

Heller,A. (2004) *Phys. Chem. Chem. Phys.*, **6**, 209–216.

Hernandez,K., and Fernández-Lafuente,R. (2011) *Enzyme Microb. Technol*., **48**, 107-122.

Hinterdorfer,P., Baumgartner,W., Gruber,H.J., Schilcher,K., Schindler,H. (1996) *Proc. Natl. Acad. Sci. USA*, **93**, 3477–3481.

Hong,M.Y., Lee,D. and Kim,H.S. (2005) *Anal. Chem.*, **77**, 7326–7334.

Horcas,I., Fernandez,R., Gomez-Rodriguez,J.M., Colchero,J., Gomez-Herrero,J. and Baro,A.M. (2007) *Rev. Sci. Instrum.*, **78**, 013705.

Huang,W., Wang,J.Q., Bhattacharyya,D. and Bachas,L.G. (1997) *Anal. Chem.*, **69**, 4601-4607.

Hutter,J.L. and Bechhoefer,J. (1993) *Rev. Sci. Instrum.*, **64**, 1868–1873.

Ikeda,T., Hata,Y., Ninomiya,K.I., Ikura,Y., Takeguchi,K., Aoyagi,S., Hirota,R. and Kuroda,A. (2009) *Anal. Biochem.*, **385**, 132–137.

Jelesarov,I. and Bosshard,H.R. (1994) *Biochemistry*, **33**, 13321-13328.

Jung,Y., Jeong,J.Y. and Chung,B.H. (2008) *Analyst*, **133**, 697–701.

Kausaite-Minkstimiene,A., Ramanaviciene,A., Kirlyte,J. and Ramanavicius,A. (2010) *Anal. Chem.*, **82**, 6401–6408.

Kwon,S.J., Lee,M.Y., Ku,B., Sherman,D.H. and Dordick,J.S. (2007) *ACS Chem. Biol.*, **2**, 419-425.

Leger,C. and Bertrand,P. (2008) *Chem. Rev.*, **108**, 2379–2438.

Lyubchenko,Y.L., Shlyakhtenko,L.S. and Gall,A.A. (2009) *Methods Mol. Biol*., **543**, 337-351.

MacBeath,G. and Schreiber,S.L. (2000) *Science*, **289**, 1760–1763.

Marko,J.F. and Siggia,E.D. (1995) *Macromolecules*, **28**, 8759-8770.

Martínez-Júlvez,M, Medina,M and Gómez-Moreno,C (1999) *J. Biol. Inorg. Chem.*, **4**, 568-578.

Martínez-Júlvez,M., Nogués,I., Faro,M., Hurley,J.K., Brodie,T.B., Mayoral,T., Sanz-Aparicio,J., Hermoso,J.A., Stankovich,M.T., Medina,M. *et al*. (2001) *J. Biol. Chem.*, **276**, 27498-27510.

Medina,M. and Gómez-Moreno,C. (2004) *Photosynth. Res.*, **79**, 113-131.

Medina,M., Martínez-Júlvez,M., Hurley,J.K., Tollin,G. and Gómez-Moreno,C. (1998) *Biochemistry*, **37**, 2715-2728.

Merkel,R., Nassoy,P., Leung,A., Ritchie,K. and Evans,E. (1999) *Nature*, **497**, 50-53.

Peregrina,J.R., Lans,I. and Medina,M. (2012) *Eur. Biophys. J.*, **41**, 117-128.

Peregrina,J.R., Sánchez-Azqueta,A., Herguedas,B., Martínez-Júlvez,M. and Medina,M. (2010) *Biochim. Biophys. Acta*, **1797**, 1638-1646.

Rodriguez-Devora,J.I., Shi,Z.D. and Xu,T. (2011) *Biotechnol. J*., **6**, 1454-1465.

Rogers,L.J. (1987) In Fay,P. and Van Baalen,C. (eds.), *The cyanobacteria*. Elsevier, Amsterdam, pp 35-67.

Roy,R., Hohng,S. and Ha,T. (2008) *Nat. Methods*, **5**, 507–516.

Sevecka,M. and MacBeath,G. (2006) *Nat. Methods*, **3**, 825–831.

Sotres,J., Lostao,A., Gómez-Moreno,C. and Baró,A.M. (2007) *Ultramicroscopy*, **107**, 1207-1212.

Sotres,J., Lostao,A., Wildling,L., Ebner,A., Gómez-Moreno,C., Gruber,H.J., Hinterdorfer,P. and Baró,A.M. (2008*) ChemPhysChem*, **9**, 590-599.

Tao,S.C. and Zhu,H. (2006) *Nat. Biotechnol.*, **24**, 1253–1254.

Volcke,C., Gandhiraman,R.P., Gubala,V., Doyle,C., Fonder,G., Thiry,P.A., Cafolla,A.T., James,B., David,E. and Williams,D.E. (2010) *J. Colloid. Interf. Sci.*, **348**, 322–328.

Wang,X., Zhou,D., Sinniah,K., Clarke,C., Birch,L., Li,H., Rayment,T. and Abell,C. (2006) *Langmuir*, **22**, 887-892.

Willner,I. and Katz,E.A. (2000) *Angew. Chem. Int. Edit.*, **39**, 1180–1218.

Wolf-Yadlin,A., Sevecka,M. and MacBeath,G. (2009) *Curr. Opin. Chem. Biol.*, **13**, 398-405.

Zhu,M., Lerum,M.Z. and Chen,W. (2012) *Langmuir*, **28**, 416–423.

Table I. Kinetic parameters of FNR-PDP for cytochrome *c* reductase activity

Immobilized on mica			
Amount of FNR in incubation mixture (μg)		Activity x10^4 (μmols/min)	TN[b] (s^{-1})
FNR_c-PDP	FNR_r-PDP		
0.16[a]	-	1.86	3.2
	0.15[a]	0.16	0.3
0.27[a,]	-	3.14	5.4
	0.30[a]	0.51	0.9
0.74[a]		4.13	7.1
1.53		4.36	7.5
3.05		5.81	10.0
6.42		4.59	7.9
10.14		4.82	8.3
11.67		3.89	6.7

In solution		
TN[c] (s^{-1})		
No tagged	FNR_c-PDP	FNR_r-PDP
17.3	18.3	5.5

[a] No saturation of FNR onto mica was theoretically achieved

[b] Turnover number (TN) values were calculated using an estimation of 3,5 x 10^{-2} immobilized μg of FNR per cm^2. The measurements are referred to 1 cm^2 of a mica sheet.

[c] TN values obtained with 4 nM of final concentration of FNR

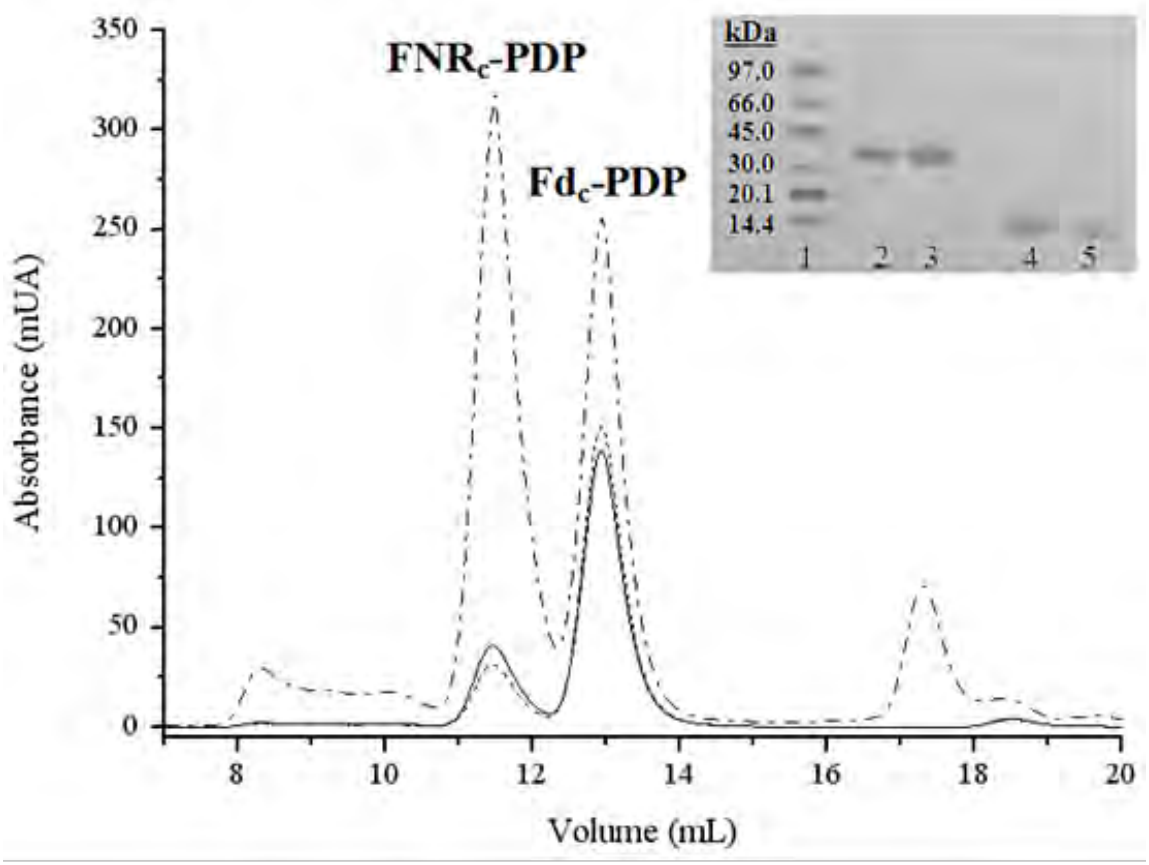

Fig. 1. Chromatogram of the separation of the tagged FNR_c:Fd_c complex through a Superdex 75 column eluting with 50 mM Tris-HCl, pH 8, 250 mM NaCl. Absorbance at 278 nm appears as a dash-dot line, at 458 nm as a continuous line and at 422 nm as a dashed line. SDS-PAGE showing the purity of the collected products appears in the inset. Line 1 shows protein markers; lines 2 and 3 show FNR_c-PDP at different concentrations; lines 4 and 5 show Fd_c-PDP at different concentrations.

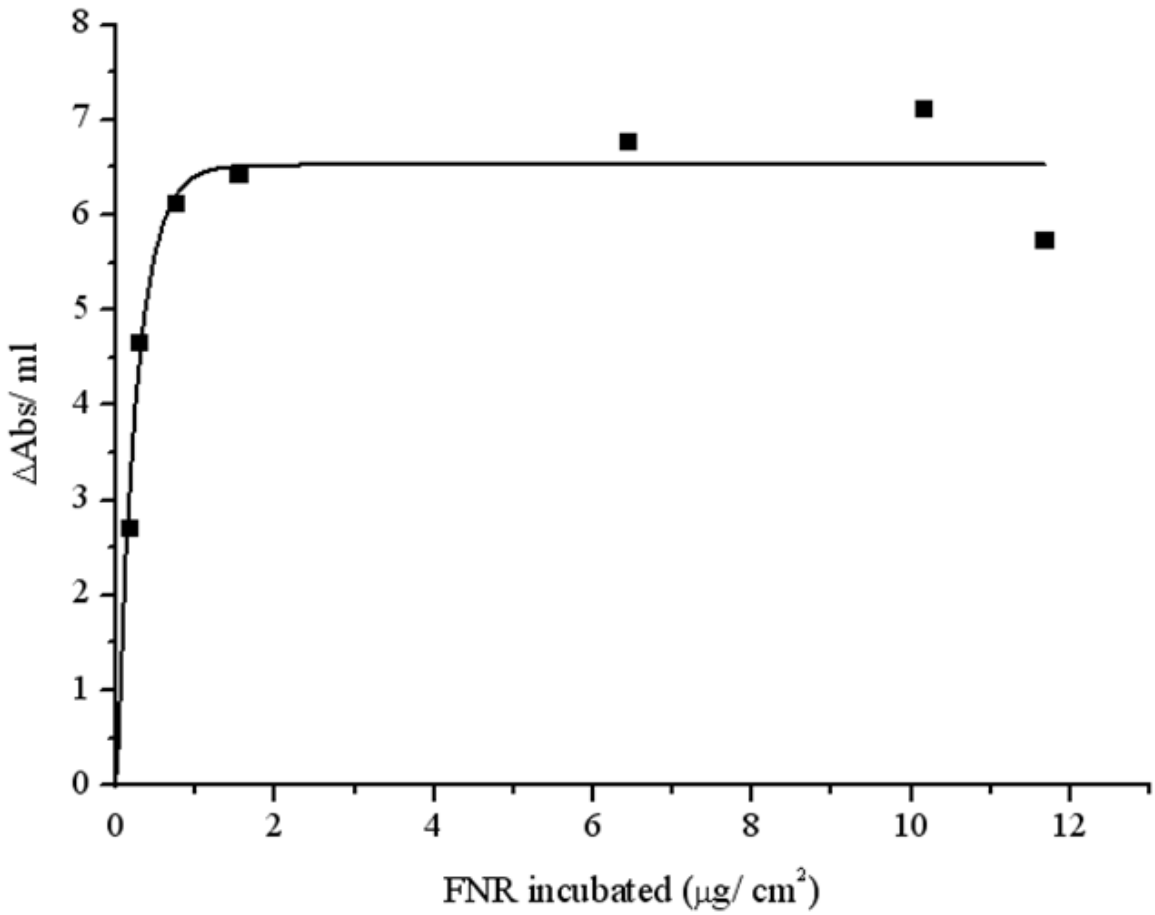

Fig. 2. Cytochrome *c* reductase activity on FNR_c mica samples. Variation of absorbance at 550 nm per volume for several amounts of incubated enzyme per surface unit.

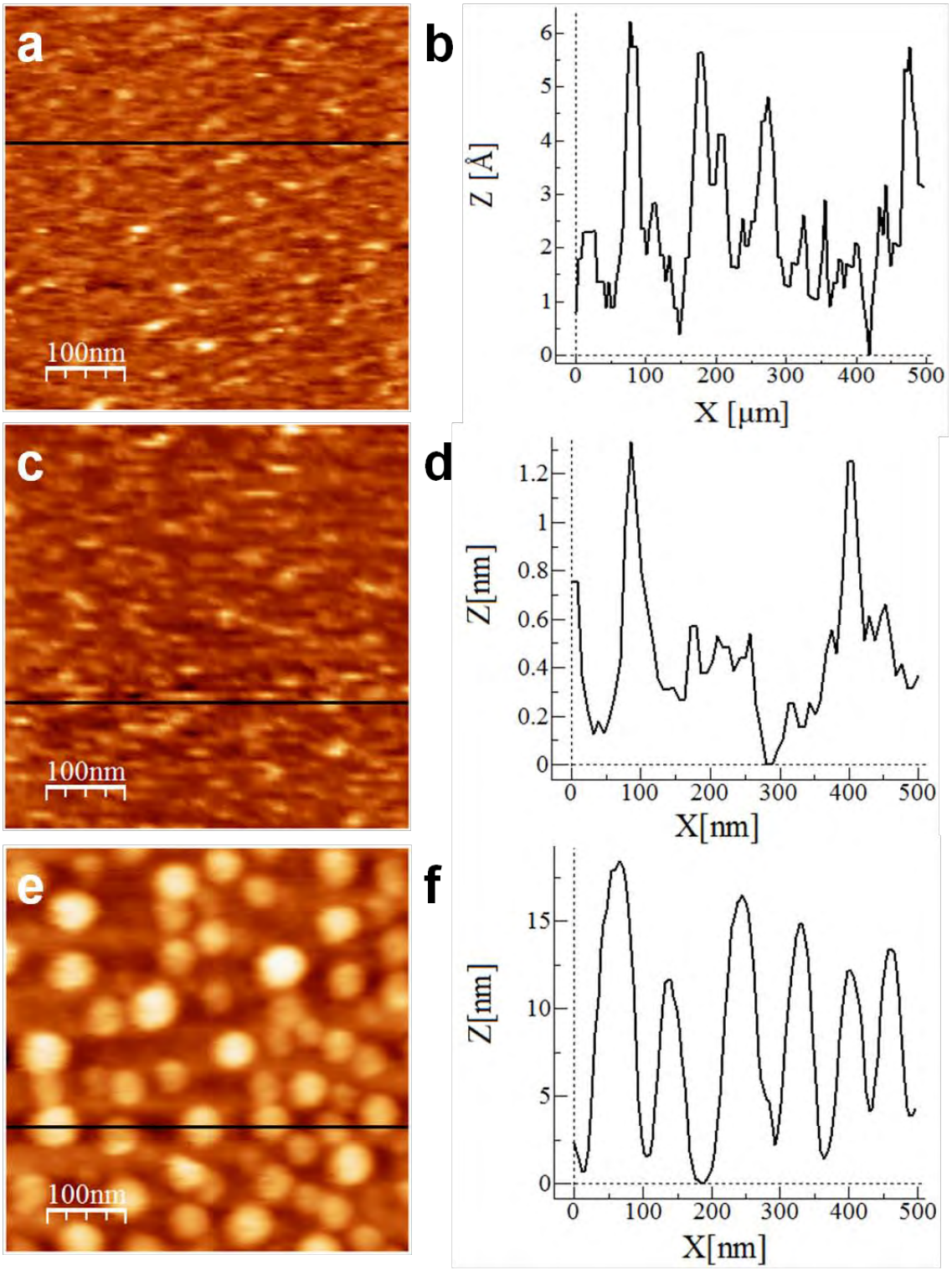

Fig. 3. JM AFM topographic images of a) APTES-modified mica and b) profile of the line of image in a) showing a height of around 0.6 nm; c) thiolated-modified mica and d) profile of the line of image in c) showing a height of around 1.2 nm; e) distribution of FNR_c covalently bound on mica and f) profile of the line of image in e) showing an average height of around 10 nm. The images showing bound FNR randomly tagged are very similar (not shown).

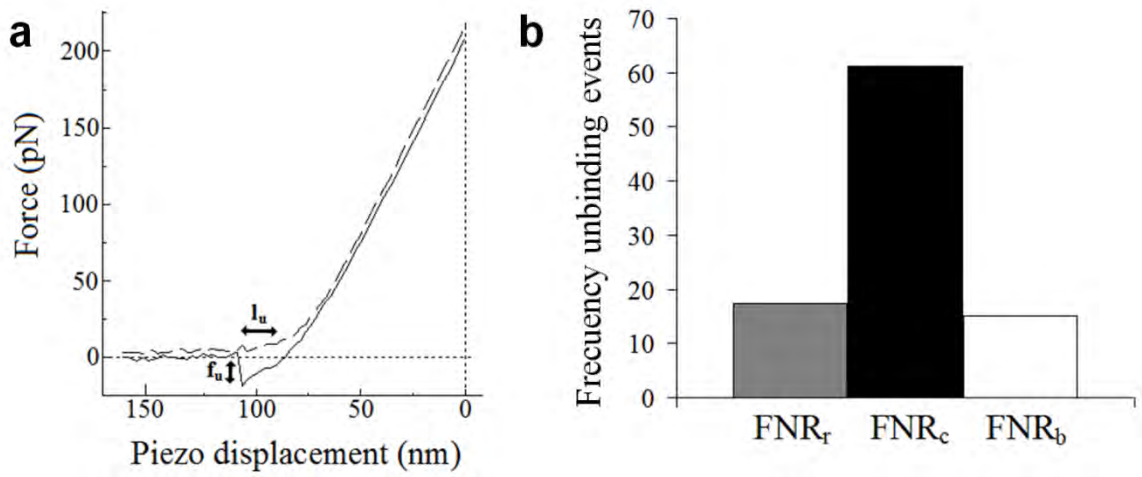

Fig. 4. a) Force curve showing a single specific rupture event for a FNR:Fd complex. Molecules are brought into binding contact when the sample is moved upward approaching the tip (dashed line). During the down movement retraction is produced and the solid line shows the force required for unbinding (f_u) that is proportional to the cantilever deflection. The total tether length at which unbinding occurs is defined as unbinding length (l_u). b) Percentages of rupture events in the formation of FNR-Fd complexes. Black bar data obtained using FNR_c samples; gray bar shows results for FNR_r samples; white bars obtained using blocked FNR_c samples.

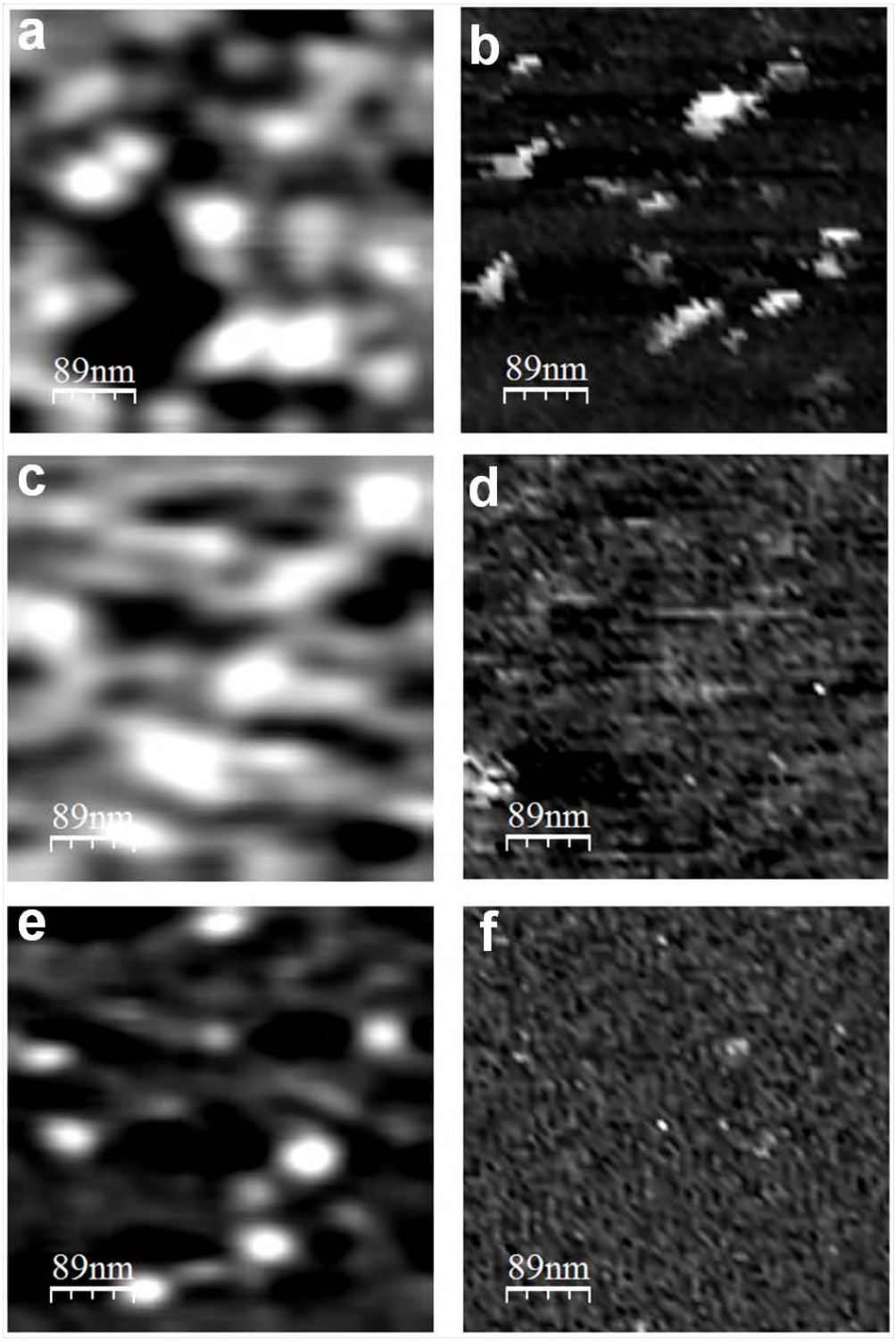

Fig. 5. Simultaneous a) topography and b) adhesion maps of a FNR_c sample. Single FNR molecules are resolved in the topography map. The high adhesion peaks in the adhesion map are due to molecular recognition events. Blocking effect after addition of free Fld into the imaging liquid cell is shown simultaneously in c) topography and d) adhesion maps. Recognition is blocked as deduced from the lack of adhesion peaks in the adhesion map. Simultaneous e) topography and f) adhesion image of a FNR_r sample. The z-axis height varies from 0 nm (black) to 8 nm (white) in the topography images. The adhesion force scale varies from 0 pN (black) to 74 pN (white) in the adhesion images. The measurements were taken in PBS using JM with functionalized Fd-tips at a scanning rate of 190 pixel s^{-1}.